[For publication in J. Nuclear Science and Technology, as the proceedings of "Actinides 2001, held in Hayama, Japan, November 4-9, 2001"]

Vibrational Raman and Optical Studies of Cm in Zirconia-based Pyrochlores and Related Oxides Matrices*

Z. Assefa', R. G. Haire[1], and P.E. Raison[2]

'Oak Ridge National Laboratory, Chemical Sciences Division, The Trans-uranium Research Group, Oak Ridge, TN 3783 l-6375.

[2]Commissariat à l'Energie Atomique, CEA-Cadarache DRN/DEC/SPUA/LACA 13 10%France.

[*Sponsored by the Division of Chemical Sciences, Geosciences and Biosciences, BES, US Dept. of Energy, under contract DE-AC05-00OR22725 with ORNL, managed & operated by UT-Battelle, LLC and Commissariat à l'Energie Atomique and Electricit de France.]

Vibrational Raman & Optical Studies of Cm in Zirconia-based Pyrochlores and Related Oxide Matrices.

Z. ASSEFA[1*], R. G. HAIRE[1], and P. E. RAISON[2]

'Oak Ridge National Laboratory, MS 6375, Oak Ridge, TN 37831-6375.
[2]Commissariat à l'Energie Atomique, CEA- DRN/DEC/SPUA/LACA 13108-Cadarache, France.

Raman spectroscopy has been employed to follow the phase behavior of Cm-Zr oxide materials as a function of Cm:Zr ratio. Three different structural phases, monoclinic, cubic and pyrochlore, are formed when the Cm:Zr ratio is varied from >0 to 1. Each phase produces a distinct Raman profile in the 100-700 cm^{-1} spectral region. Up to 10 atom % Cm, the Raman spectra indicate that the monoclinic structure is dominant. Raman bands corresponding to the monoclinic phase are absent in samples containing 20 - 40 atom % Cm. Concomitantly, a band at -600 cm' broadens and increases in intensity with increasing curium content, indicating that the cubic phase is dominant in this concentration range. The pyrochlore oxide structure, which forms at 50 atom % Cm, generates three Raman bands (the center of mass are at 283, 387,495 cm-') out of six bands predicted by nuclear site group analyses. The strongest of these is at 283 cm-', and corresponds to the O-Cm-O bending mode. Details of these studies will be compared and discussed with data obtained for comparable systems containing selected analogous 4f-elements.

Keywords: ***vibrational Raman, pyrochlore-oxides, actinide, curium.***

1. Introduction

Zirconia-based oxide ceramics are attractive for a variety of applications, such as fuel cells, oxygen sensors, refractory materials, and in nuclear waste disposal schemes' . [3)]. Several attributes influence the physical and chemical properties of these materials, which include crystal structures, type and level of dopant, as well as temperature[4)]. Pure ZrO_2 is known to exist in three polymorphic phases (monoclinic, tetragonal or cubic), with the more symmetrical phases being obtained with increasing temperature. Doping zirconia with different cations' can stabilize the cubic and tetragonal phases at lower or ambient temperatures. This stabilization improves important mechanical and electrical properties of ZrO_2. In this regard, lanthanide dopants in zirconia are known to stabilize the tetragonal and/or cubic crystal phases[6 - 8)] over temperature ranges pertinent to catalytic reactions. The phase transitions are known to follow a non-diffusion pathway and involve displacements of oxygen atoms in the unit cells[9)].

The main structural difference among these different zirconia phases is due to slight displacements of oxygen atoms in the unit cell. Thus, Raman spectroscopy can be used as a probe to follow the changes and become an important complement to X-ray diffraction. This combined approach of study is important for two reasons: first, oxygen-cation vibrations dominate the Raman spectrum, while the X-ray diffraction patterns are influenced more by the heavy metal ions. Therefore, oxygen displacements may be probed better by the vibrational Raman technique. Secondly, oxygen vibrations rising from the dopant can be probed separately from those of the host cations by the vibrational Raman technique.

In this study, we have employed Raman spectroscopy to follow phases in the ZrO_2 hosts, as a function of Cm:Zr ratio. The results are compared with data from Sm-Zr materials to allow us to assess the effects of ionic size and/or radioactivity on the formation of the different phases. The luminescence properties of these systems have also been studied, and the formations of defect types associated with these phases have been established; details of the latter will be reported elsewhere.

II.Experimental

The starting materials were commercial, high-purity ZrO_2 and Sm_2O_3 (both 99.9 %). The "^{248}Cm isotope" (actually, 97 % Cm-248 and 3 % Cm-246) used in these experiments was made available by the U.S. Department of Energy through its heavy element production program at the Oak Ridge National Laboratory.

Sample preparations were made by mixing appropriate quantities of aqueous solutions of each component, drying and then calcining the solids up to 1775 K in air for -20 hours. The aqueous solutions were prepared from zirconyl nitrate, $Sm(NO_3)_3*6H_2O$, and $CmCl_3$. Products were characterized by X-ray diffraction using 114.6 mm Debye-Scherrer cameras (Mo $\lambda_{K\alpha 1,2}$ = 0.71073 Å radiation). The

*Corresponding author
Tel. (865) 574-5013; Fax (865) 574-4987
E-mail: assefaz@ornl.gov

cell parameters for the pyrochlore system were refined by a least squares method. For monoclinic and cubic phases the data were compared with literature diffraction profiles. The full details of the X-ray diffraction studies are presented separately in this volume").

Raman studies were conducted on the same samples that were probed by X-ray diffraction. The 457 nm argon-ion (Coherent, model 306) laser line was used for excitation. A double-meter spectrometer (Jobin-Yvon Ramanor model HG.2S) with a resolution of 0.5 cm" at 514.5 nm was used. The samples' signals were detected by a photon counting system, which employed a photo-multiplier tube (Hamamatsu R636) and a multi-channel analyzer (Nicolet 1170) interfaced with a PC. Data analyses were conducted with Grams32 software (Galactic, version 5.1). Additional optical studies were conducted using an Instrument SA's optical system that consists of a monochromator (model 1000M) in conjunction with CCD, PMT and IR detectors.

III. Results and Discussion

In Figure 1 are shown the Raman spectra of ZrO_2 samples, as a function of the Sm content. The undoped ZrO_2 spectrum (Figure la) has sharp bands that are characteristic of the monoclinic phase (space group C_{2h}^5). The unit cell consists of four molecules and all four of the Zr nuclei occupy a "4e"

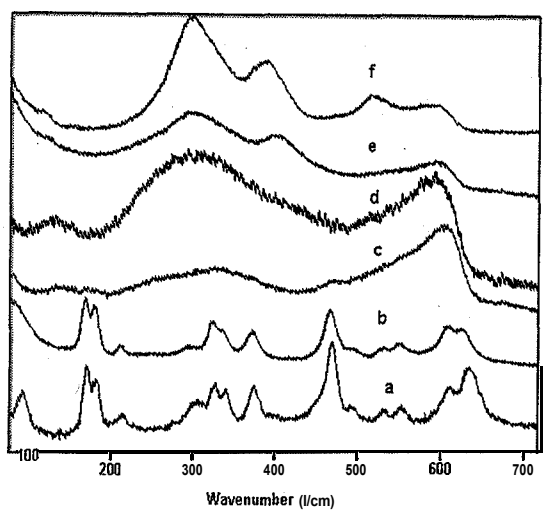

Fig.1 Raman spectra: a) m-ZrO_2; b) $Sm_{0.1}Zr_{0.9}O_{1.95}$; c) $Sm_{0.2}Zr_{0.8}O_{1.9}$;d) $Sm_{0.3}Zr_{0.7}O_{1.85}$; e) $Sm_{0.4}Zr_{0.6}O_{1.8}$; f) $Sm_2Zr_2O_7$.

Wyckoff site with C, site-symmetry"). The eight oxygen nuclei in this unit cell also occupy two crystallographically distinguishable "4e" sites of C, symmetry. Nuclear site group analysis of this structure predicts 18 Raman active bands of $9A_g + 9B_g$ modes, where the most intense are observed (Figure la) at 176, 190, 3 11, 332, 345, 379,475, 6 12, and 63 9 cm^{-1}. At 10 % Sm substitution of the Zr atoms, the Raman spectrum (Figure lb) has a similar profile with that of monoclinic, m-ZrO_2 (Figure la). These similarities are indicative of the dominance of the monoclinic phase up to at least 10 % Sm substitution. Nevertheless, some minor changes are evident in the lb spectrum, which includes a shift of the 639 doublet peak to 629 cm-'. Raman bands assignable to pure Sm_2O_3 (monoclinic phase) are not observed in the spectrum, indicating that Sm replaces Zr nuclei in the matrix. Such replacements must be accompanied by the creation of charge compensating vacancies on the anion sites[12].

Figure 1c shows the Raman profile for 20 % Sm^{3+} doping. For this composition, all of the characteristic bands of the monoclinic phase are absent, while a broad band peaking at 607 cm^{-1} (FWHH, full width at half height = 78 cm") is dominant. The latter band is typically displayed by the cubic ZrO_2 phase[9]. Nuclear site group analysis for cubic ZrO_2 (space group O_h^5) predicts a very simple vibrational spectrum, consisting of one Raman-active phonon band of a T_{2g} symmetry. The spectrum shown in Figure Id (30 % Sm), in addition to the characteristic broad band of the cubic phase at 607 cm", consists of broad feature at -330 cm-' (FWHH = 130 cm-'). This latter band becomes more symmetrical, and its relative intensity increases, as the Sm content is increased. At 40 % Sm substitution (Figure 1e), the band at -600 cm^{-1} is significantly reduced. In addition, a broad shoulder at -402 cm^{-1} emerges with a concomitant increase in the intensity of the band at -306 cm-'. This spectrum is representative of a zirconia sample in which the cubic and pyrochlore structures coexist. The results obtained from the Raman studies are consistent with the X-ray data (details of the X-ray studies are presented in this volume along with the various phase relationships")).

As seen in Figure If, the pyrochlore structure produces a well-defined Raman profile at a 1: 1 (Sm:Zr) ratio. Four of the six Raman bands predicted by nuclear site group analysis of the pyrochlore structure (space group O_h^7, z= 8) are observed at 302, 397, 522, and 596 cm^{-1}(FWHH = 56, 37, 30, and 39 cm-', respectively).

The Raman spectra exhibited by the Cm-Zr samples are shown in Figure 2. The spectral profiles are similar to those described for the Sm-Zr system. Comparison of Figures 2a and 2b indicates that at 10 % Cm substitution, the Raman spectrum closely resembles that of monoclinic ZrO_2. As is the case with Sm-Zr samples, the monoclinic phase is dominant at 10 % Cm doping. The presence of other phases may be inferred from the spectral profile shown'in Figure 2c, where features of the monoclinic phase appear to persist up to at least 20 % Cm content, although the relative intensities indicate a change in symmetry. The band at 6 15 cm-' (Figure 2c) has now broadened and increased in intensity. Between 20 and 30 % Cm substitution, the vibrational features characteristic of themonoclinic phase have diminished, while the asymmetric broad band in the vicinity of 600 cm^{-1} has become dominant. The band corresponds to the single T_{2g} mode expected for the cubic phase. The broadness and

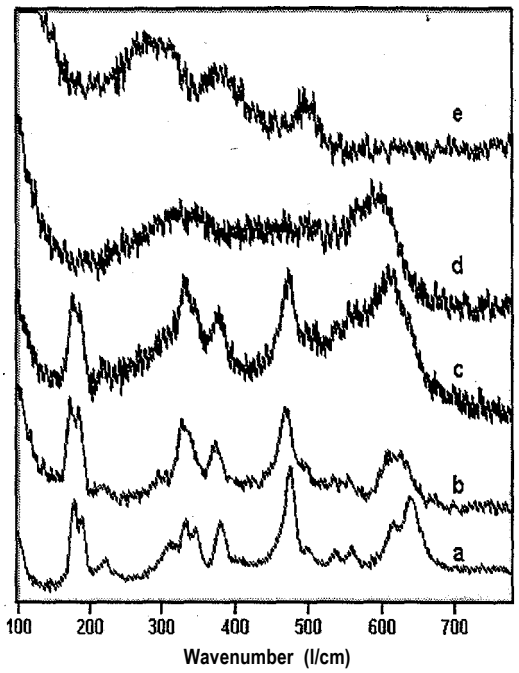

Fig. 2 Raman spectra of ZrO_2:Cm(III): a) m-ZrO_2; b) $Cm_{0.1}Zr_{0.9}O_{1.95}$; c) $Cm_{0.2}Zr_{0.8}O_{1.9}$; d) $Cm_{0.3}Zr_{0.7}O_{1.85}$; e) $Cm_2Zr_2O_7$

asymmetry of this band point to disorder within the oxygen lattice, recognized as arising from oxygen vacancies[13].

At a 1: 1 (Cm:Zr) ratio, the Raman profile (Figure 2e) exhibits bands that best correspond to the pyrochlore structure. From these data it can be inferred that curium exists in a trivalent oxidation state, although the tetravalent state is known (as in e.g.,CmO_2)[14]. Moreover tetravalent actinide dopants in ZrO_2 systems have also been noted previously[15]. However, curium(IV) is not stable at higher temperatures, and the Cm(III) appears "locked-in" by the stabilizing nature of the pyrochlore structure. In the 20-50 % Cm substitution ranges, it is believed that Cm(III) stabilizes the cubic form of ZrO_2, much like Y(III) does (e.g., the so-called YSCZ, yttrium stabilized cubic zirconia)[3].

Three well-defined bands are observed in the Cm-Zr oxide system (four in the Sm-Zr system) compared to the six Raman bands predicted by nuclear site group analysis. These bands have their centers of mass at 283, 387, 495 (FWHH= 95, 52, and 29 cm-', respectively). The strongest peak is observed at 283 cm^{-1} and corresponds to the O-Cm-O bending mode. This band is significantly broader than the corresponding Sm-Zr system (FWHH = 95 vs. 56 cm-' in the Cm- and Sm-Zr systems, respectively). Moreover, the Raman peaks of $Cm_2Zr_2O_7$ are shifted to lower frequencies when compared to those in the Sm-pyrochlore system. The band corresponding to the 0-Sm-0 bending mode is observed at 302 cm-', while the corresponding O-Cm-O mode is red shifted by -20 cm^{-1} and appears at 283 cm-'. The decrease in the phonon frequencies of the Cm-pyrochlore, as compared to the Sm-pyrochlore, is consistent with the mass difference between the two nuclei.

IV. Structure vs Raman in Pyrochlores

The Zr-f-element pyrochlore oxide structure has a cubic unit cell (space group Fd3m, O_h^7) with lattice constants of ~ 10 Å[16] and has eight molecules in the unit cell. In a perfect pyrochlore structure, all of the 16 Ln or An cations in the unit cell would reside at the c-site and have D_{3d} site symmetry: The 16 Zr nuclei would then occupy a crystallographically distinct d-site but have a similar D_{3d} site symmetry. A nuclear site-group analysis of this structure indicates that each of the two sets of nuclei contribute $A_{,,} + E_u + 2T_{1u} + T_{2u}$ to the total vibrational modes. However, none of these modes is Raman active, as the cations reside on inversion centers. The 56 oxygen atoms in the unit cell occupy two distinct crystallographic sites. The f-site, with C_{2v} site symmetry, is occupied by 48 oxygen atoms, and their contribution to the total vibrational modes is $A_{1g}+A_{2u}+E_g + E_u + 2T_{1g}+ 3T_{2g}+ 3T_{1u} + 2T_{2u}$. The remaining eight oxygen nuclei occupy the a-site, with a T_d site symmetry, and have $T_{1u} + T_{2g}$ contribution to the total vibrational modes. Of these oxygen atom vibrational contributions, only the $A_{,,} + E_g + 4T_{2g}$ modes are Raman active. Hence a total of six Raman bands, which are related to vibration of the anion substructure, are expected in the pyrochlore system.

Four of these expected six Raman bands were observed in the Sm- and three in the Cm-Zr pyrochlore oxide systems, The Raman bands exhibited by the Cm-pyrochlore are broader than those recorded from the Smpyrochlore system. One reason may be due to the smaller sample sizes used in the studies of the Cm-pyrochlore. In addition the Raman signal could be affected by randomly oriented vacancies that may distort long-range ordering.

Although the pyrochlore structure consists of ordered oxygen vacancies at the 8b crystallographic site, several studies have indicated the existence of various degrees of anion disorder in this structure. A line broadening correlation between ionic conductivity and anion disorder has been established previously"'. Hence, the Raman profile could reflect the degree of disorder in these systems. For example, the large broadening exhibited by the Cm-Zr system, as compared to the Sm-Zr pyrochlore, could imply a higher degree of disorder in the former. Defect formation is a known source of structural disorder and break-down of translational symmetry, resulting in broadening of the Raman vibrational profile. In the pyrochlore materials, the size and oxidation states of substitutional ions are known to introduce vacancies and create defects[18]. Radioactivity (especially the neutron emissions) from the Cm is an additional factor that could introduce defects and result in the broadening of the Raman profile[19]. The defect centers created by oxygen

vacancies provided orange-red luminescence from the Cm system at -645 nm. The details of the photo-luminescence study are beyond the scope of this paper and will be reported elsewhere[20].

V. Conclusion

Raman spectroscopy has been employed in this work to follow successfully the phase behavior of Cm-Zr and Sm-Zr oxide materials as a function of the Cm:Zr and Sm:Zr ratios. Although determination of the exact compositional location of the phase boundary would require study at smaller incremental compositions, we have identified broad ranges in which the three phases exist. In the Cm:Zr ratio from >0 to 1, each phase provides a distinct Raman profile iri the 100 - 700 cm^{-1} spectral region. The cubic phase is identified by its characteristic broad band at -600 cm" for the compositional region of 20-40 % substitution. The pyrochlore structure, formed at 50 atom % Cm, shows three Raman bands (at 283, 387, and 495) out of the six predicted by nuclear site group analyses. The strongest of these bands is located at 283 cm" and corresponds to the O-Cm-O bending mode. The Raman profile for the monoclinic phase is more complex given the lower symmetry of this phase.

Acknowledgement

This research was sponsored by the Division of Chemical Sciences, Geosciences and Biosciences, Office of Basic Energy Sciences, US Department of Energy, under contract DE-AC05-00OR22725 with Oak Ridge National Laboratory, managed by UT-Battelle, LLC. P. E. R also acknowledges support from the Commissariat à l'Energie Atomique and Electricit de France.

References

1) E. C. Subbarao, H. S. Maiti, Adv. Ceram. 24, 731, (1988).
2) D. Yuan, F. A. Kroger, J. Electrochem. Soc. 116,594, (1996).
3) M. S. Isaacs, "Science and Technology of Zirconia, Advances in Ceramics" A. H. Heuer, L. W. Hobbs, (Eds), American Ceramic Society, Columbus, OH, 406, (1981).
4) M. Maczka, E.T.G. Lutz, H. J. Verbeek, K. Oskam, A. Meijerink, J. Hanuza, J. Phys. Chem. Solids 60, 1909, (1999).
5) M. C. Caracoche, P. C. Rivas, A. P. Pasquevich, A. R. L.' Garcia, J. Mater. Res. 8, 605, (1993).
6) D. J. Kim, H. J. Jung, J. Am. Ceram. Soc. 76, 2106, (1993).
7) G. Morell, R. S. Katiyar, D. Torres, S. E. Paje, J. Llopis, J. Appl. Phys. 81, 2830, (1997).
8) F. A. Mumpton, R. Roy, J. Am. Ceram. Soc. 43, 234, (1960).
9) M. Yashima, K. Ohtake, M. Kakihana, H. Arashi, M. Yoshimura, J.Phys. Chem. Solids 57, 17, (1994).
10) P.E. Raison, R. G. Haire, Z. Assefa (to appear in this volume)
11) D. L. Rousseau, R. P. Bauman, S. P. S. Porto, J. Raman Spectr. 10,253, (198 1).
12) C. M. Phillippi, K. S. Maazdiyasni, J. Am. Ceram. Soc. 54, 254, (1971).
13) D. W. Liu, C. H. Perry, A. A. Feinberg, Phys. Rev. B51, 201, (1995).
14) R. G. Haire, Z. Assefa, N. Stump, Mat. Res. Soc. Proc. 506, 153, (1998).
15) P.E. Raison, R. G. Haire, T. Sato, T. Ogawa, Mat. Res. Soc. Proc. 556, 3, (1999).
16) M. A. Subramanian, G. Aravamudan, G. V. S. Rao, Prog. Solid St. Chem. 15, 55, (1983).
17) R. E. Williford, W. J. Weber, R. Devanatban, J. D. Gale, J. Electra-ceramics 3 (4), 409, (1999).
18) M.Oueslati, M. Blakanski, P. K. Moon, H. L. Tuller, Mat. Res. Soc. Symp. Proc. Vol. 135,199, (1989).
19) Z. Assefa, R. G. Haire, "Nuclear Site Remediation" P. G. Eller, W. R. Heineman (Eds), ACS Symposium Series, 778 (Chapter 20), 329, (2001).
20) Z. Assefa, R. G. Haire, P. E. Raison (to be submitted).